



**HAL**  
open science

# Miniaturized affinity chromatography: A powerful technique for the isolation of high affinity GAGs sequences prior to their identification by MALDI-TOF MS

Frédéric Jeanroy, Clothilde Comby-Zerbino, Claire Demesmay, Vincent Dugas

► **To cite this version:**

Frédéric Jeanroy, Clothilde Comby-Zerbino, Claire Demesmay, Vincent Dugas. Miniaturized affinity chromatography: A powerful technique for the isolation of high affinity GAGs sequences prior to their identification by MALDI-TOF MS. *Analytica Chimica Acta*, 2023, 1277, pp.341656. 10.1016/j.aca.2023.341656 . hal-04184392

**HAL Id: hal-04184392**

**<https://hal.science/hal-04184392>**

Submitted on 21 Aug 2023

**HAL** is a multi-disciplinary open access archive for the deposit and dissemination of scientific research documents, whether they are published or not. The documents may come from teaching and research institutions in France or abroad, or from public or private research centers.

L'archive ouverte pluridisciplinaire **HAL**, est destinée au dépôt et à la diffusion de documents scientifiques de niveau recherche, publiés ou non, émanant des établissements d'enseignement et de recherche français ou étrangers, des laboratoires publics ou privés.

# **Miniaturized affinity chromatography: a powerful technique for the isolation of high affinity GAGs sequences prior to their identification by MALDI-TOF MS**

Frédéric Jeanroy<sup>1</sup>, Clothilde Comby-Zerbino<sup>2</sup>, Claire Demesmay<sup>1</sup>, Vincent Dugas<sup>1,\*</sup>

<sup>1</sup> *Université de Lyon, CNRS, Université Claude Bernard Lyon 1, Institut des Sciences Analytiques, UMR 5280, 5 rue de la Doua, F-69100, Villeurbanne, France*

<sup>2</sup> *Université de Lyon, CNRS, Université Claude Bernard Lyon 1, CNRS, Institut Lumière Matière UMR 5306, F-69100, Villeurbanne, France*

\* Corresponding author. Tel.: +33437423552

E-mail address: vincent.dugas@univ-lyon1.fr

**Keywords:** Frontal Affinity Chromatography, Miniaturization, Glycosaminoglycans, Antithrombin III, MALDI-TOF MS.

## Abstract

Glycosaminoglycans (GAGS) are involved in many biological processes through interactions with a variety of proteins, including proteases, growth factors, cytokines, chemokines and adhesion molecules. Identifying druggable GAG-protein interactions for therapeutic purposes is a challenge for the analytical community. In this context, this work investigates the use of a new miniaturized monolithic affinity column (poly(GMA-co-MBA) grafted with antithrombin III (AT III) to specifically capture and elute high affinity sequences contained in low molecular weight heparin (enoxaparin) for further on-line characterisation. This miniaturized, high binding capacity affinity column allows the specific capture of high-affinity oligosaccharide chains from Enoxaparin, even at low concentrations and with a minimal consumption of AT III. In addition to purification, this elution process enables preconcentration for direct analysis by capillary zone electrophoresis. It was found that many of oligosaccharide chains in enoxaparin were eliminated and that certain chain sequences were retained and enriched. Direct coupling with MALDI-TOF MS was successfully used to further characterize the specifically retained oligosaccharides where nano-ESI-TOF MS failed. After optimisation of the sample preparation and ionisation parameters, direct on-line analysis was performed by applying the elution volume released from the miniaturized affinity column ( $\leq 1 \mu\text{L}$ ) directly to the MALDI plate. Finally, this original miniaturized analytical workflow coupling miniaturized AT III-affinity chromatography to MALDI-TOF MS detection is able to select, enrich and detect and identify high affinity sequences (mainly DP4 in size length with a high degree of sulfation) from low molecular weight heparin samples. A more specific selection of GAG sequences can be achieved by increasing the ionic strength during the washing step of affinity chromatography. This is consistent with the known binding pattern between heparin and AT III.

## 1. INTRODUCTION

Glycosaminoglycans (GAGs) are linear and highly negatively charged polysaccharides abundantly found at the cell surface and in the extra-cellular matrix of animal cell [1]. GAGs structure is built out of repeating disaccharides units which are the combination of an uronic acid (iduronic acid IdoA or glucuronic acid GlcA) and an hexosamine (N-AcetylGalactosamine GalNAc or N-AcetylGlucosamine GlcNAc) [2]. Thus, GAGs are divided into six families which can be distinguished based on the nature of these disaccharide blocks: chondroitin sulfate (CS), dermatan sulfate (DS), heparan sulfate (HS), heparin (HP), and keratan sulfate (KS). During the last decades, their role has emerged to be essential in various physiological and pathological contexts such as neurodegenerative diseases, angiogenesis, cancer and pathogen infections [3,4]. This great diversity of function relies on specific GAG–protein interactions. Deciphering the sugar code [5] of such GAG–protein interaction is therefore of great interest. Ultimately, elucidating the structure-function relationship by determining the GAG ligand structure could enable the design of GAG-like drugs for potential therapeutic applications [6].

While many GAG-binding sites of proteins have been identified [7,8], breaking the protein binding site of GAG remain a real challenge due to the structural diversity of GAGs [9]. The best known and probably most studied interaction is the binding between Heparin and Antithrombin, involved in blood coagulation processes. It took almost a decade from the mid-1970s to identify the GAG motif, namely a pentasaccharide as the binding pattern [10] using a battery of powerful analytical techniques (affinity chromatography, NMR). To our knowledge, no other protein-binding pattern has been unambiguously identified. Indeed, GAGs structure present a large structural diversity due to different sulfation rate, epimerization... Furthermore, GAGs are generally found in heterogeneous mixtures of several polysaccharides with different sizes and structures from 9 to over 20 000 disaccharides units [1,11]. Thus, multiple sequences may have affinity for a given protein.

Therefore, identification of the major binding pattern is a tremendous analytical challenge and requires multidisciplinary approach.

To achieve this ambitious goal, different approaches have emerged in recent years, involving isolation, enrichment and sequencing of the binding pattern. Filter-entrapment has been proposed by Yu et al. [12] while solid-phase supported have been explored by Keiser et al. with the use of surface non-covalent affinity-mass spectrometry (SNA-MS) [13] or by Przybilsky et al. with surface plasmon resonance imaging (SPRi) [6], both of them coupled with MALDI-TOF. Another top-down approach implying enzymatic depolymerisation of Heparin after binding to AT III and detection by size exclusion chromatography coupled with mass spectrometry has been presented by Niu et al. [14]. Finally, complete analytical workflow based on affinity chromatography have been used to elucidate new specific binding domain sequences in the development of novel GAG-based therapeutics [15-16]. However, there is still room for improvement in the development of alternative approaches that combine the use of low sample volumes with increased sensitivity. Recently, the use of miniaturized affinity chromatography coupled with mass spectrometry (nanoESI-TOF) has been proposed in order to specifically capture and elute high affinity AT III-binding site sequence in a complex oligosaccharide mixture. This strategy has the advantage of 1) reducing protein consumption due to the miniaturized scale and 2) improving the surface-area-to-volume ratio compared to flat solid supports, thereby increasing the amount of specific oligosaccharide captured [17]. Like other existing strategies, this approach involves the use of low molecular weight heparin (LMWH) derivatized from unfractionated heparin (UFH) by controlled chemical or enzymatic depolymerisation. Enoxaparin is one of the most commonly used LMWHs and is obtained by alkaline depolymerisation of UFH, resulting in an unsaturated uronic acid residue at its non-reducing ends and 1,6-anhydroaminosugars at a small fraction of its reducing ends [18]. In-line coupling of Antithrombin III-functionalized miniaturized affinity columns with nanoESI-MS was used to detect, the high-affinity pentasaccharide (Fondaparinux), selectively captured among a complex mixture of low

molecular weight heparin. This was the proof of concept for the selective capture and release strategy of high-affinity sequences. However, due to multiple-charge states, alkali metal ions heterogeneity ( $\text{Na}^+/\text{H}^+$  and  $\text{Na}^+/\text{K}^+$  exchanges) and ion suppression [19], enoxaparin chains are not detected by nanoESI-MS without an upstream separation technique [17] and the selective capture of high-affinity enoxaparin sequences could not have been demonstrated yet. In fact, a much greater challenge is posed by the identification and selection of enoxaparin sequences. On the one hand, the interaction sequence with AT III may be absent below its minimum size and only present on a large chain that is difficult to detect by MS techniques. On the other hand, the interaction sequence is present in very small amounts in this type of mixture.

Capillary zone electrophoresis (CZE) [20,21], reversed-phase liquid chromatography (RPLC) [22], strong anion exchange chromatography (SAX) [23] or hydrophilic interaction liquid chromatography (HILIC) [24,25] are usually used for separating GAGs mixture preventing ion suppression before ESI-MS detection. Otherwise, another way to detect GAGs mixture by mass spectrometry is to use of matrix assisted laser desorption/ionization (MALDI). This technique presents the advantage to produce singly charged ions [26] resulting in an improved sensitivity.

In this study, we investigate the use of a miniaturized monolithic AT III-affinity column for the selective capture and direct detection of high-affinity enoxaparin-AT III chains in minute amounts of sample of Low Molecular Weight Heparin (LMWH). This type of very complex and very heterogeneous mixtures has been used in other strategies to identify interaction sequences [30]. These strategies have highlighted the difficulty of identifying the pentasaccharide interaction sequence with AT III, which is present at very low levels and potentially on large oligosaccharides that are difficult to detect. Thus, even if the process of capture, selection and release of fondaparinux added to an LMWH mixture has been demonstrated, the detection and identification of unknown sequences selected on an affinity column within such a mixture is a much more challenging task.

Here, we demonstrate the ability of nano-affinity chromatography to capture and preconcentrate specific oligosaccharides contained in an enoxaparin mixture into a small aqueous sample elution volume (sub- $\mu\text{L}$  to 1  $\mu\text{L}$ ). In addition, a new poly(GMA-co-MBA) monolith synthesized at miniaturized scale is used for the first time for oligosaccharides capture and elution application. This new monolith has a higher maximum binding capacity allowing higher enrichment factors to be achieved without non-specific interactions which is critical in this application. Analysis of the captured/released sequences by capillary zone electrophoresis (CZE), a miniaturized high-resolution separation technique, highlights the selective aspect of the strategy and allows the fingerprinting of LMWH samples before and after the selective capture step. It turns out that the elimination of a large proportion of the oligosaccharide sequences originally present in enoxaparin, with the selection and enrichment of a small number of very specific enoxaparin chains, can be achieved at the miniaturized scale by affinity chromatography on an AT III capillary column. Further characterization was performed by MALDI-TOF MS to identify enoxaparin sequences released from the column without intermediate step involving chromatographic separation of the eluted mixture, which to our knowledge has never been achieved with an affinity chromatography strategy. This coupling set configuration between the nanoaffinity column and the MALDI-TOF MS detection system is made possible by optimizing the elution step. Elution from the affinity column is triggered by injecting a small plug of 0.1 M ammonia solution, which is applied directly onto the MALDI plate for mass detection and characterization. A detailed study of the mass spectra shows the selectivity of the capture and allows the identification of the main sequences with high affinity for antithrombin.

## **2. MATERIALS AND METHODS**

### **2.1. Chemicals**

Ethylene dimethacrylate (EDMA, 97%), glycidyl methacrylate (GMA, 98%), acrylamide, N,N'-Methylenebis(acrylamide) (MBA), 1-propanol, 1,4-butanediol, (3-methacryloxypropyl)-trimethoxysilane ( $\gamma$ -MAPS), methanol (HPLC grade), triethylamine (TEA), pentylamine (PTA), 1,1,1,3,3,3-Hexafluoro-2-propanol (HFIP), sodium periodate, lithium hydroxide, dipotassium hydrogen phosphate ( $K_2HPO_4$ ), o-phosphoric acid, acetic acid, sodium cyanoborohydride, 2-(4-Hydroxyphenylazo)benzoic acid (HABA), 1,1,3,3-tetramethylguanidine (TMG), Fondaparinux (FDPX) sodium and Enoxaparin sodium were purchased from Sigma-aldrich (Saint-quentin Fallavier, France), ammonia solution (28-30 %) was purchased from Merck (Darmstadt, Germany), sulfuric acid (18 M) from VWR (Fontenay-sous-bois, France). All aqueous solutions were prepared using  $> 18 M\Omega$  deionized water. Preparation of the phosphate buffer was done by dissolving 1.17 g of  $K_2HPO_4$  in 100 mL of ultrapure water and pH was adjusted to 7.4 with o-phosphoric acid.

## 2.2. Instrumentation

Capillary monolithic columns were prepared using a pressure gradient microfluidic flow controller MFCS-EZ100 system (Fluigent, Villejuif, France) to handle liquids inside the capillary. Inlet pressure values are reported to specify the liquid flow conditions (outlet pressure was always set up at atmospheric pressure). An LC pump L-6000 (Merck, Darmstadt, Germany) was used to rinse the freshly prepared monolithic capillary columns.

Nano-FAC-UV experiments (frontal affinity chromatography experiments) and CZE-UV (capillary electrophoresis experiments) were carried out with a capillary electrophoresis Agilent 7100 system (Agilent Technologies, Waldbronn, Germany) equipped with an external pressure nitrogen supply allowing to work up to 12 bars (up to  $0.1 \text{ cm s}^{-1}$  with aqueous solutions for a 8.5 cm monolith). The affinity experiments were carried out in the pressurization mode (by applying external pressure on the outlet vial, no voltage applied) with the CE system in the "short-end" injection mode. The detection was achieved "on-column" (in an empty section of the 10-cm capillary located just after the monolith), with a diode array detector operated in a multi-wavelength mode. For affinity experiment, the

effective length of the affinity column was 8.5 cm. System control and data acquisition were carried out using the Chemstation software (Agilent). The carousel and cassette temperatures were set at 25°C. After each analysis, the capillary column was rinsed with 20 column volumes of phosphate buffered solution.

Nano-FAC-TOF-MS analyses were carried out with a Nano-LC 400 system (Eksigent) connected to TOFMS analyzer (Agilent 6230 TOF LC/MS) using an nano-electrospray ionization source. An additional make-up flow (300 nL min<sup>-1</sup>) was added with the loading pump of the nano-LC device and mixed with the chromatographic flow in a zero-dead volume union (UH-750 from IDEX (Cluzeau info labo, France). Nanospray stainless steel emitters with a uniform 30 µm-inner diameter were purchased from Pepsep (Marslev, Denmark).

MALDI-TOFMS experiments were carried out with a MALDI-TOF MS (UltrafleXtreme from Bruker) equipped with a 355 nm Smartbeam II laser with a 19 kV acceleration voltage and a 20 kV reflection voltage. MS data were acquired in the negative reflector ion mode and externally calibrated with a standard solution of fondaparinux. Samples were deposited on a MTP AnchorChip target plate (from Bruker).

### **2.3. Preparation and characterization of AT III affinity columns**

Two types of monolithic columns were used: columns with a poly(GMA-co-EDMA) monolithic stationary phase (75 µm inner diameter) synthesized in UV-transparent capillaries for UV detection purposes and columns with a poly(GMA-co-MBA) monolithic stationary phase prepared in polyimide-coated fused-silica capillaries (150 µm inner diameter) for other experiments.

All the capillaries were pre-treated (1 h at 700 mbar) with a 5 % (v/v) solution of γ-MAPS in methanol/water (95/5, v/v) 2.5 % TEA for 1h. Next, they were rinsed with methanol for 15 min at 700 mbar and dried at room temperature under nitrogen stream.

#### **2.3.1. Synthesis of poly(GMA-co-EDMA) monolith**

Fused-silica capillaries with UV transparent coating (TSH, 75- $\mu\text{m}$  i.d.) were purchased from Polymicro Technologies (Molex, France). poly(GMA-co-EDMA) monoliths were synthesized as described in a previous work [27]. A polymerization mixture is prepared by mixing 0.9 mL GMA, 0.3 mL EDMA, 1.05 mL 1-propanol, 0.6 mL 1,4-butanediol, 0.15 mL ultra-pure water and 12 mg of AIBN initiator. The  $\gamma$ -MAPS pre-treated capillary is then filled with the polymerization mixture under 100 mbar  $\text{N}_2$  pressure. The photopolymerization reaction is performed in a Bio-link UV cross-linker (VWR International, France) under 365 nm UV light for a total energy of 6  $\text{J cm}^{-2}$ . To localize the monolith inside the silica capillary, a PEEK tubing (380  $\mu\text{m}$  i.d.) is used as a mask to cover non-irradiated areas. After polymerization, the 8.5-cm monolithic segment of the 15-cm capillary (column volume of 375 nL) is rinsed with methanol for 1 h with a chromatographic pump (30 bars).

### **2.3.2. Synthesis of poly(GMA-co-MBA) monoliths**

Poly(GMA-co-MBA) monoliths are prepared as follows adapting protocol from [28,29] in fused-silica capillaries with polyimide external coating (TSP, 150- $\mu\text{m}$  i.d. purchased from Polymicro Technologies (Molex, France)). A polymerization mixture is prepared by mixing 0.48 g GMA, 0.32 g MBA, 3.33g DMSO, 1.85 g dodecanol, 1.48 g 1,4-butanediol, and 8 mg of AIBN initiator. The pre-treated capillary is then filled with the polymerization mixture under 1 bar  $\text{N}_2$  pressure and the ends of the capillary sealed. The polymerization reaction is performed in water bath at 57  $^{\circ}\text{C}$  for 18 hours. After polymerization monoliths are rinsed with methanol for 1 h.

### **2.3.3. Covalent grafting of AT III onto GMA-based monolith (Schiff base method)**

First, the epoxy groups of the monoliths are hydrolyzed into diols by flowing 1 M sulfuric acid solution for 2 h at 700 mbar. After rinsing, the diol moieties are oxidized into aldehyde ones using a 0.12 M  $\text{NaIO}_4$  solution at pH 5.5. Then, a solution containing AT III (1  $\text{mg mL}^{-1}$ ), Fondaparinux (at 170  $\mu\text{M}$  to completely saturate the heparin binding sites of AT III) and  $\text{NaBH}_3\text{CN}$  (4  $\text{mg mL}^{-1}$ ) is prepared in phosphate buffer (67 mM pH 6) and percolated through

the column for 18 h at 0.7 MPa at room temperature (dynamic grafting). After AT III immobilization, the column is flushed (2 h, 0.7 MPa) with sodium borohydride ( $\text{NaBH}_4$  at  $2.5 \text{ mg mL}^{-1}$  in phosphate buffer 67 mM pH 8) to reduce residual aldehydes. The affinity columns are then rinsed with phosphate buffer and stored at  $4^\circ\text{C}$ . The columns grafted in presence of fondaparinux (FDPX), are thoroughly rinsed with ammoniac 0.1M (pH 11) to remove FDPX from AT III before any use.

#### 2.3.4. Characterization of the AT III columns by nano-FAC-TOF MS

For each type of column, the number of AT III active binding sites ( $B_{\text{act, AT III}}$ ) was determined by nano-FAC-TOFMS experiments using a  $5 \mu\text{M}$  FDPX solution in ammonium acetate solution (20 mM, pH 7.4). Considering the high affinity between FDPX and AT III ( $K_d$  in the nM range) and the high FDPX concentration (in the  $\mu\text{M}$  range) with respect to the  $K_d$  value, it can be assumed that the column is saturated at this concentration. Thus, the number of active binding sites can be estimated in a single experiment according to equation 1:

$$B_{\text{act,ATIII}} = (t_{\text{plateau}} - t_0) \times F \times [\text{FDPX}] \quad (\text{equation 1})$$

with  $F$  being the flow rate and  $t_0$  the column hold-up time,  $t_{\text{plateau}}$  the breakthrough time of FDPX.

#### 2.4. Capture and elution of AT III high-affinity GAG oligosaccharides

Affinitive oligosaccharide sequences are captured in frontal affinity mode using solutions of enoxaparin at  $200 \mu\text{M}$  and  $2 \mu\text{M}$  (medium concentration), chondroitin sulfate at  $200 \mu\text{M}$ , fondaparinux at  $5 \mu\text{M}$  and mixtures of enoxaparin/chondroitin sulfate at  $200 \mu\text{M} / 200 \mu\text{M}$  and enoxaparin/fondaparinux at  $200 \mu\text{M} / 5 \mu\text{M}$ . Solutions were prepared in 67 mM phosphate buffer pH 7.4 (UV-Vis detection) or in 20 mM ammonium acetate buffer pH 7.4 (MS detection). The infusion is stopped when the breakthrough curve is observed (with UV detection for enoxaparin and TOF-MS detection for Fondaparinux). To remove any residual GAG oligosaccharides with low affinity to AT III (at the end of the capture step), the columns are rinsed with the capture buffer (20 to 30 dead volumes as indicated in the text). The

specifically captured GAG-oligosaccharide structures are then eluted by injection of 0.1M ammonia (pH 11) (1  $\mu$ L).

For capillary electrophoresis analysis, ten elutions from AT III-functionalized poly(GMA-co-EDMA) monolithic capillary column (8.5 cm in length) are pooled. Finally, a solvent exchange was performed by evaporating the ammonia and recovering it in 10  $\mu$ L of ultrapure water before injection.

For MALDI-TOF analysis, the elution is done through a 10-cm length poly(GMA-co-MBA) monolith functionalized with AT III (150  $\mu$ m i.d.) directly onto the MALDI plate.

## **2.5. Analysis of captured/released AT III high-affinity GAG oligosaccharides by capillary zone electrophoresis and UV detection.**

Enoxaparin analyses by capillary zone electrophoresis were adapted from [30] and performed in 50 mM phosphate buffer pH 3.5 in a fused silica capillary of 71.5 / 63 cm (total length / effective length) and 75  $\mu$ m internal diameter. Analyses are performed in negative polarity with an applied voltage of -20 kV. Electrokinetic injection is performed by applying a voltage of -10 kV for 10 seconds. Detection wavelength is set at 232 nm. The enoxaparin standard (without capture/release step) is prepared in water at a total concentration of 10  $\mu$ M and 2  $\mu$ M. The electroosmotic mobility ( $0.45 \cdot 10^{-4} \text{ cm}^2 \text{ s}^{-1} \text{ V}^{-1}$ ) was measured according to the method developed by Vigh et al [31].

## **2.6. Analysis of captured/released oligosaccharide sequences by MALDI-TOF MS**

The MALDI plate is an AnchroChip plate. The matrix used is a (HABA/TMG) matrix (1/2) prepared at 80 mg mL<sup>-1</sup> in methanol as in previous works [32–34]. The HABA/TMG mixture is ultrasonicated for 15 minutes. The solution is then evaporated overnight and made up to 80 mg mL<sup>-1</sup> in methanol. An amount of 100  $\mu$ M NaCl was added to prevent desulfation phenomena [32]. The spot of target is coated with 0.5  $\mu$ L of vacuum-dried matrix and then with 1  $\mu$ L of vacuum-dried sample. The released samples are collected at the outlet of the column to 1  $\mu$ L and then applied directly to the MALDI target before drying under vacuum.

## 3. Results

### 3.1. Specification of the AT III affinity monolithic columns

Poly(GMA-co-EDMA)-based monolithic capillary columns were initially used based on their widespread use in affinity chromatography. 10-cm length monolithic columns are *in-situ* synthesized by photoinitiated polymerization in UV-transparent capillaries fused silica capillaries (75- $\mu\text{m}$  inner diameter (i.d.)). AT III grafting by the Schiff base method results in poly(GMA-co-EDMA) monolithic columns with an amount of binding sites ( $B_{\text{act, AT III}}$ ) of  $1.3 \pm 0.2 \text{ pmol cm}^{-1}$  i.e. about  $13 \pm 2 \text{ pmol per column (n=3)}$ ). Efforts to increase the binding capacity motivated the development and use of an improved monolithic column. We recently reported the development of a more hydrophilic poly(GMA-co-MBA) monolith. This new monolith has interesting properties for the present application as it combines different surface properties compared to the monolith used previously. It has a more pronounced hydrophilic character which makes it possible to limit possible non-specific interactions by hydrophobic effect, and a more important ( $B_{\text{act}}$ ) capacity. Finally, this monolith is obtained by thermal polymerization which makes it possible to work in capillaries with a larger internal diameter (UV-transparent capillaries being commercially limited to 100- $\mu\text{m}$  i.d.). For comparison purpose, ( $B_{\text{act, AT III}}$ ) of  $1.7 \pm 0.3 \text{ pmol cm}^{-1}$  are obtained in 75- $\mu\text{m}$  i.d. capillaries and up to  $6.3 \pm 0.8 \text{ pmol cm}^{-1}$  in 150- $\mu\text{m}$  i.d. capillaries. More information about the properties of monoliths is presented in supplementary material (*1-Columns characterization and properties*).

Regarding the condition of use of these AT III monolithic capillary columns, the capture and elution process using ammonia solution under the defined conditions can be repeated successively many times without significant loss of active binding sites. This elution process is demonstrated to be quantitative even with high affinity ligands (such as FDPX) (see supplementary material : *2-Columns stability*).

### **3.2. Ability of AT III capillary monolithic columns to specifically capture high affinity oligosaccharide sequences in a LMWH mixture**

To demonstrate the selective capture of GAG oligosaccharides in a mixture of low molecular weight heparin (LMWH), the capture/release protocol was first applied to enoxaparin. Enoxaparin is composed of depolymerized sequences of Heparin of various sizes and sulfation patterns. The Antithrombin interaction site is likely to be present but on large sequences ( $dp > 6$ ) and therefore difficult to detect by ESI-MS. However, the presence of unsaturation at the non-reducing end allows UV detection. This investigation was done using UV-transparent poly(GMA-co-EDMA) monolithic column and in-situ UV detection. A sample of enoxaparin was percolated onto the AT III affinity column until its breakthrough from the column. The column was then washed with increasing volumes of percolation buffer (phosphate buffer) to remove non-retained or weakly retained oligosaccharide sequences. Oligosaccharides strongly retained by AT III were then eluted by percolation of a 0.1 M ammonia solution (suppression of amine ionization of the protein and hence of electrostatic interactions between the protein and the anionic oligosaccharides). The capture and release steps were in-line monitored by UV absorption spectrometry at 232 nm, using monolithic capillary affinity columns installed in a capillary electrophoresis device operated in pressurized mode (Figure 1 A).

Regardless of the duration of the wash step (up to 16 column volumes), an elution peak is still observed at the beginning of the elution step, corresponding to the release of

oligosaccharide sequences from the AT III column. The miniaturized AT III affinity column is expected to strongly retain sequences with high-affinity for AT III. The decrease in peak area with increasing washing step duration shows that the more extensive the wash, the more efficient the removal of low affinity sequences. However, as there is no separation step, no further information can be drawn on the number and type of sequences selectively captured and released.

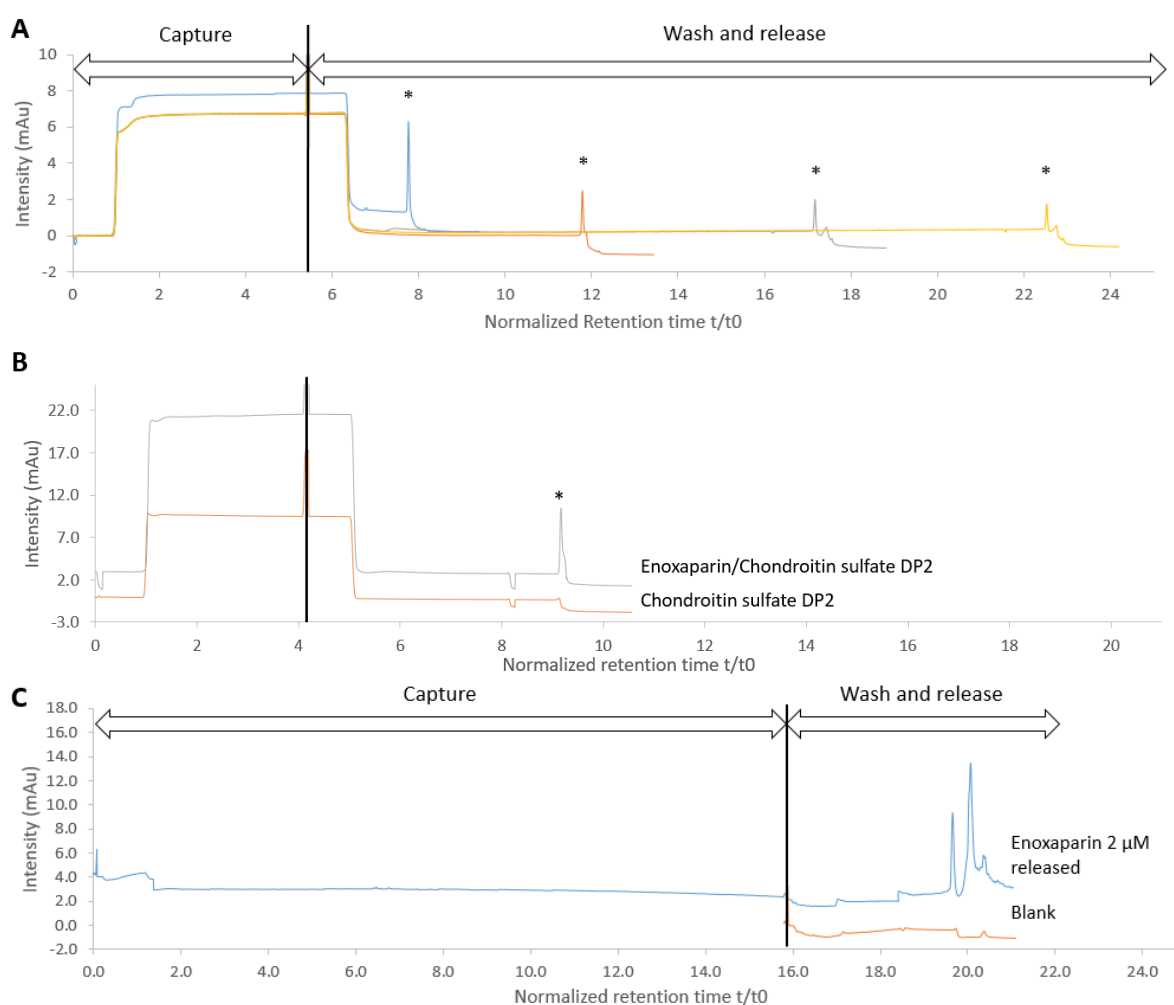


Figure 1: Capture/wash/elution processes on a 8.5 cm length AT III poly(GMA-co-EDMA) monolithic capillary column with and a UV detection at 232 nm of A: Enoxaparin 200 μM with 2 column volumes of washing (blue line), 5 column volumes of washing (orange line), 10 column volumes of washing (grey line) and 16 column volumes of washing (yellow line). B: Chondroitin sulfate DP2 200 μM (orange line) and Enoxaparin/Chondroitin sulfate DP2 200 μM/200 μM mixture (grey line) C: Enoxaparin 2 μM (blue line) and a blank (orange line)

To demonstrate the specificity of the capture, the protocol was then applied to a sample of chondroitin sulfate (monosulfated disaccharide), which has no known affinity for AT III but

also carries a negative charge. Comparison of the capture/wash and ammonia release traces (Figure 1 B) obtained for enoxaparin and chondroitin sulfate samples clearly shows the absence of a peak during the release phase with chondroitin sulfate. This shows that washing conditions suppress the retention of loaded compounds that do not have a specific and high affinity for AT III. Finally, when enoxaparin was percolated in a mixture with chondroitin sulfate, oligosaccharides of enoxaparin were still captured and detected in the released phase. This shows that the presence of non-affinity compounds with the same charge as sequences with affinity for AT III does not prevent the capture and release of these sequences.

Finally, a sample of enoxaparin at low concentration (2  $\mu\text{M}$ ) was percolated to demonstrate the ability of miniaturized AT III monolithic column to preconcentrate high-affinity enoxaparin compounds (Figure 1 C). Due to the low concentration of enoxaparin sample (below limit of detection), the capture step did not show any breakthrough curve usually observed in FAC when equilibrium is reached. However, compared to the blank experiment, a signal attributed to enriched enoxaparin oligosaccharides is observed during the elution step with ammonia 0.1M and after washing with 3 column volumes. This result illustrates the enrichment capacity of the affinity column for high-affinity sequences even at low concentration.

These results demonstrate the selective capture of oligosaccharide sequences from LMWH samples by affinity with AT III and their release in low ionic strength aqueous solution (0.1M ammonia). This result also shows that, given the washing volume, the eluted sequences have a high affinity for AT III. However, with UV detection, it is impossible to know their number or structure. Moreover, an online detection by ESI-MS showed that the sequences were not detected, due to their low concentrations and the presence of multiple adducts. However, this elution process makes this method compatible to direct coupling to other analytical methods (i.e electrokinetic separation methods and MALDI mass spectrometry) contrarily to standard high ionic strength elution methods (NaCl in the molar range).

### **3.3. Analysis of enoxaparin oligosaccharide sequences from AT III monolithic column by capillary zone electrophoresis and UV detection**

Of importance is the analysis of the oligosaccharide composition of the captured and eluted enoxaparin fraction. Since enoxaparin is a very complex mixture of oligosaccharides the introduction of a separation step should allow to demonstrate the ability of the AT III affinity column to specifically select sequences of interest from a complex mixture. The use of chromatographic techniques such as SAX or HILIC are techniques often used offline to separate and analyze mixtures of oligosaccharides. However, these techniques are difficult to adapt to volumes eluted at a miniaturized scale (approximately 1  $\mu$ L). The choice of capillary electrophoresis is justified by its intrinsic miniaturization given the minute elution volumes associated with the use of monolithic capillary columns (in the microliter range), and by its resolution power given the complexity of the mixture. In fact, capillary electrophoresis offers the possibility of separating oligosaccharides based on the relative migration velocities of oligosaccharides according to their charge/size ratio. In particular, this method allows the separation of different oligosaccharides according to the degree of sulfation, the acetylation of the carboxylic acid functions and the degree of polymerization of the oligosaccharides. The analysis of enoxaparin using the method developed by Patel et al. [30] gives a migration profile that reflects the complexity of the mixture (Figure 2, orange trace). In addition, the sensitivity is high enough to allow the study of a sample eluted from a AT III nano-column.

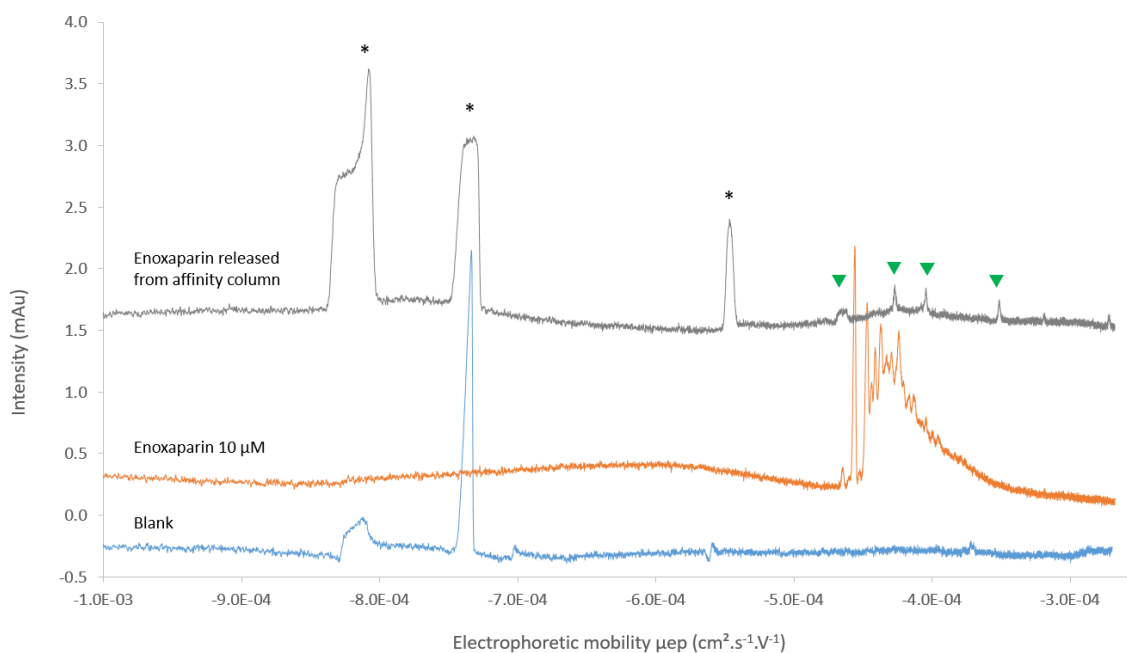


Figure 2: Electropherograms obtained with a 50 mM phosphate buffer pH 3.5 in a capillary of 71.5 cm total length and UV detection at 232 nm of Enoxaparin (orange line), Enoxaparin released from AT III poly(GMA-co-EDMA) affinity column by ammonia 0.1 M (grey line) and a blank released from affinity column (blue line). Asterisks point peaks from column or ammonia. Green arrows highlight enoxaparin peaks released after selective capture.

The comparison of the electrophoretic profiles of enoxaparin solution before and after passing through the affinity column is shown in Figure 2. A large proportion of the oligosaccharide sequences have been eliminated during the affinity step, as shown by the disappearance of the envelope peak between 4.2 and 5 minutes on the electropherogram. However, some peaks remain or are even amplified at the end of the selection process (green arrows in Figure 2). This shows that the capture step applied to a mixture of low molecular weight heparins significantly reduces sample complexity by favoring the recovery of species with high affinity for AT III. The capture step is selective and to obtain information on the identity of the selected compounds, appropriate mass spectrometry analysis is attractive. Since in-line coupling with nano-ESI-MS detection does not allow the detection of enoxaparin oligosaccharides under the analytical conditions (i.e. ion suppression and signal dilution due to multiple charge states or adducts), on-line coupling by MALDI-TOF MS analysis was considered. This coupling was chosen because of the small amount of sample

recovered after a capture and elution process and the specificity of ionization of this technique compared to ionization by electrospray.

Direct spotting of the elution solution onto the MALDI target and solvent evaporation allows concentration of the entire sample in a single spot, avoiding dilution effects (inherent in many other liquid coupling techniques) and decreasing of detection limits. In addition, MALDI ionization has the advantage of producing low-charge state ions. The production of predominantly single charge ions is a real advantage over other ionization methods in mass spectrometry, such as electrospray, because the signal is concentrated on a smaller number of ionic species per compound. This maximizes detection.

### **3.4. Analysis of oligosaccharide enoxaparin sequences eluted from miniaturized AT III monolithic column by MALDI-TOF MS**

#### **3.4.1.1. Optimization of MALDI-TOF MS detection**

Although the detection of GAG-type oligosaccharides by MALDI-TOF MS has already been described, an optimization of the analytical conditions (deposition conditions, ionization matrix, analytical conditions) was necessary to achieve the required detection performance for the on-line coupling of this technique with affinity nanocolumn. Optimization of GAG oligosaccharide analysis conditions was first performed using fondaparinux as a model. This synthetic oligosaccharide allows the preparation of solutions with a single compound. This pentasaccharide is representative (in terms of size and charge) of the oligosaccharide sequences likely to be selected on an AT III affinity column.

The main optimization criteria regarding the small amount of oligosaccharide that is expected to be recovered by the affinity chromatography step concerns the detectability of the non-desulfated forms of the GAG oligosaccharides by MALDI-TOF MS. In fact, the sulfation level of GAGs targeting AT III is known to be quite high. It is therefore necessary to define analysis conditions avoiding or limiting the desulfation of these compounds. The main operating parameters are the choice of the ionization matrix, the detection polarity mode and the laser power. Among the different matrices studied for the analysis of GAGs ( $\alpha$ -cyano-4-hydroxycinnamic acid (CHCA), 2,5-dihydroxy benzoic acid (DHB), sinapic acid), ionic liquid matrices (ILM) have been previously reported to help in ionization and suppression of fragmentation (i.e. loss of  $\text{SO}_3$ ) of highly acidic oligosaccharides [33]. A HABA/TMG matrix with a 1/2 molar ratio has been identified in previous work [33,34] as a matrix that allows a high level of sensitivity to be achieved. To mimic the release conditions of a sample from an affinity column, a volume of 1  $\mu\text{L}$  of 50  $\mu\text{M}$  fondaparinux solution prepared in water was first used to optimize the deposition conditions.

Among the various tests performed, the best deposition configuration was obtained by depositing 0.5  $\mu\text{L}$  of matrix prepared by mixing liquid ionic matrix (HABA/TMG 1:2 in 80 mg/mL methanol) with a 100  $\mu\text{M}$  NaCl solution. In the literature, the addition of NaCl is used to limit the desulfation of sulfated oligosaccharides [32], by formation of sodiated adducts that are more stable during the ionization step. Under MALDI analysis conditions, the addition of sodium has a significant effect on sensitivity. After the matrix was dried, 1  $\mu\text{L}$  of fondaparinux solution was applied to the ILM spot and allowed to dry. Each MALDI spot then contained 50 pmol fondaparinux. Positive and negative polarity tests were performed, and it appeared that even when the fully sulfated intact fondaparinux is the major compound, the sensitivity is significantly lower in the positive polarity.

The analysis of a sample of fondaparinux in HABA/TMG matrix after air drying is shown in Figure S4. Under these conditions, the intact molecular ion (without loss of sulfate) are

detected in the form of sodium and potassium adducts between 1700 th and 1800 th (see table S2 for more details) and desulfated species at lower m/z values.

These cation exchanges and loss of sulfate groups result in complex peak patterns composed of a large number of peaks for the same compound. The signal is therefore spread over a greater number of peaks per compound reducing the signal intensity and making spectrum interpretation more difficult. Various modifications of this initial protocol were considered to limit this exchange to obtain simpler spectra and improved signal intensities. Although the use of cation exchange resins makes it possible to limit this effect (Figure S4), this treatment does not seem to be easily compatible with small sample volumes (of the order of 1  $\mu$ L). Somewhat unexpectedly, the vacuum drying of the samples, which was initially used to homogenize the deposits, produced surprising results in terms of signal improvement, thus making it possible to limit this phenomenon (Figure S4). The analysis was then performed with a sample of fondaparinux prepared in a 0.1 M ammonia solution to mimic the composition of the solution at the outlet of the affinity column. The spectra obtained were comparable whether the samples were applied in water or in 0.1M ammonia (results not shown). Finally, to mimic what will happen with enoxaparin after the capture and elution step, fondaparinux (5  $\mu$ M) was percolated on a AT III monolithic affinity column until breakthrough, the column was rinsed with 40 dead volumes of percolation buffer, and the captured fraction was released directly onto the MALDI plate. The spectrum shows that after the entire process, FDPX is present at a concentration high enough to be detected by MALDI-TOF MS (Figure S5).

These optimized conditions were used for the analysis of enoxaparin by MALDI-TOF MS. Contrary to what was observed with fondaparinux alone and as illustrated Figure S6, laser power is an important parameter for the detection of oligosaccharide sequences of enoxaparin. It is important to ensure that the laser power does not become too intense, otherwise the information about the desired compounds will be lost. If the power is too high, the signal obtained no longer contains the information of the intact oligosaccharide

sequences (Figure S6). In this case, the laser induces fragmentation. The spectrum is traversed by repeated patterns at 142 Th intervals, which have not yet been identified.

The optimized conditions (laser power set at 65%) were used for the analysis of enoxaparin by MALDI-TOF-MS. First, a sample of enoxaparin prepared in water and applied to a MALDI plate at 200 pmol per spot gave the spectrum shown in Figure 3.

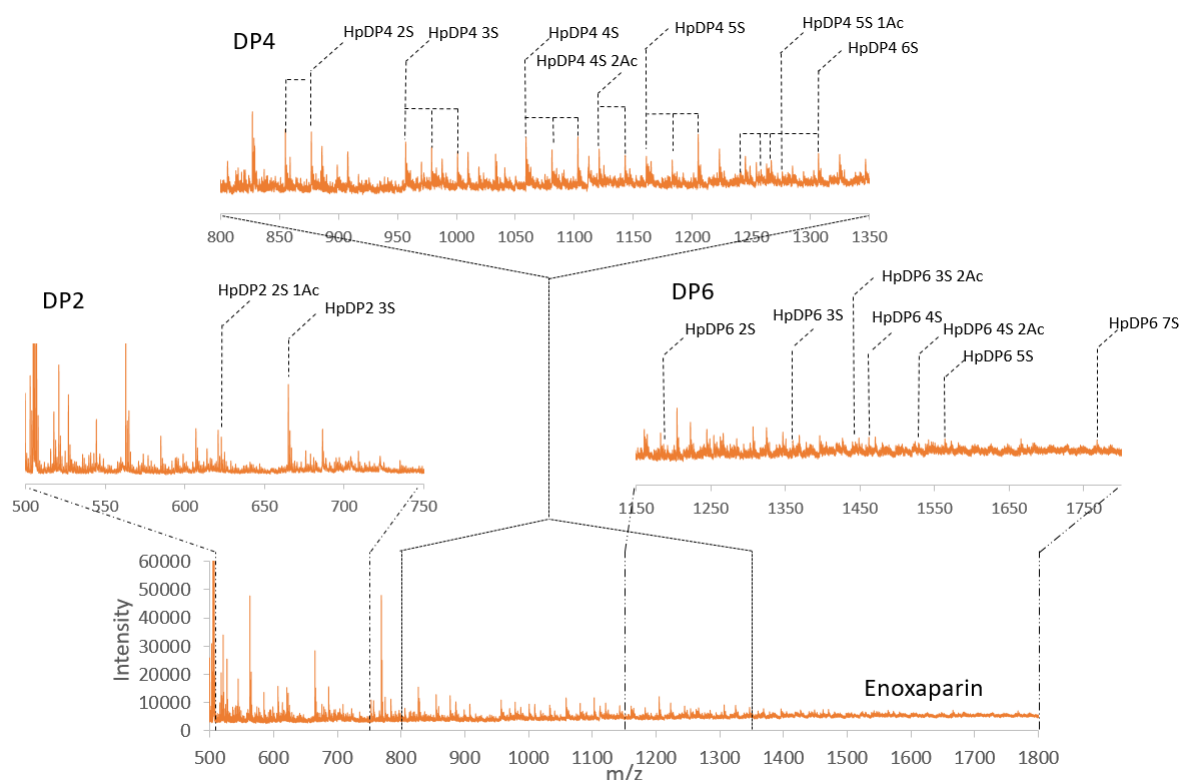


Figure 3: Negative ion reflector MALDI-TOF mass spectrum of Enoxaparin (200 pmol/spot) Highlights of DP2 range between  $m/z=500$  and  $m/z=750$ , DP4 range between  $m/z=800$  and  $m/z=1350$  and DP6 range between  $m/z=1150$  and  $m/z=1750$ . Sample were prepared with HABA/TMG  $\frac{1}{2}$  80 mg mL<sup>-1</sup> in methanol matrix and a ratio 0.5/1  $\mu$ L of matrix/sample was deposited on AnchorChip plate.

With an appropriate (sufficiently low) laser power, it is possible to detect numerous oligosaccharide sequences of DP2, DP4 or DP6 (Table 2). It should be noted that for chain sizes larger than DP6, detection becomes difficult in terms of sensitivity. Many GAG oligosaccharides from DP2 to DP6 have been identified under different adducts (sodium loss, sodium/potassium exchange, etc.). All identified oligosaccharides bear at least 2 sulfates in

their structure. It should also be noted that many signals have not yet been identified. They may be larger oligosaccharides (whose exact masses have not yet been determined) or fragments that are formed during the ionization process [26]. Indeed, it has been shown that MALDI ionization can lead to source fragmentation on oligosaccharides [35].

### **3.4.2. Analysis of AT III high-affinity enoxaparin oligosaccharides by MALDI-TOF MS**

Enoxaparin was percolated through AT III poly(GMA-co-MBA) monolithic column and eluted with ammonia directly onto the MALDI plate. In order to maximize the quantity of material eluted, the use of a newly developed monolith was chosen in order to maximize the enrichment factor for increased sensibility. As mentioned above, poly(GMA-co-MBA) monolithic column has the advantage over poly(GMA-co-EDMA) that it can be synthesized inside capillaries of higher i.d., which also improves the number of active protein binding sites [29] and thus the maximum loading capacity. Indeed, it was demonstrated that 1  $\mu$ L of elution volume is still enough to quantitatively elute the high-affinity oligosaccharide sequences captured in such higher i.d. column conditions. This combination of increased capture binding site density and increased column volume at constant elution volume compared to the poly(GMA-so-EDMA) monolith results in a significant increase in the enrichment factor (see SI).

The resulting spectrum is shown in Figure 4. The spectra comparison before and after passing through affinity column shows a significant evolution of the oligosaccharide profile, as already observed in the preliminary results obtained by CZE analysis. It should be noted that spectra profiles obtained are similar regardless of the rinsing time (between 10 and 30 minutes), with a decrease in intensity as the rinsing time increases.

Percolation of the low molecular weight heparin through the affinity column therefore allows simplification of the mixture by selecting the compounds with the strongest affinity to the AT III target protein (Figure 4, Table 1).

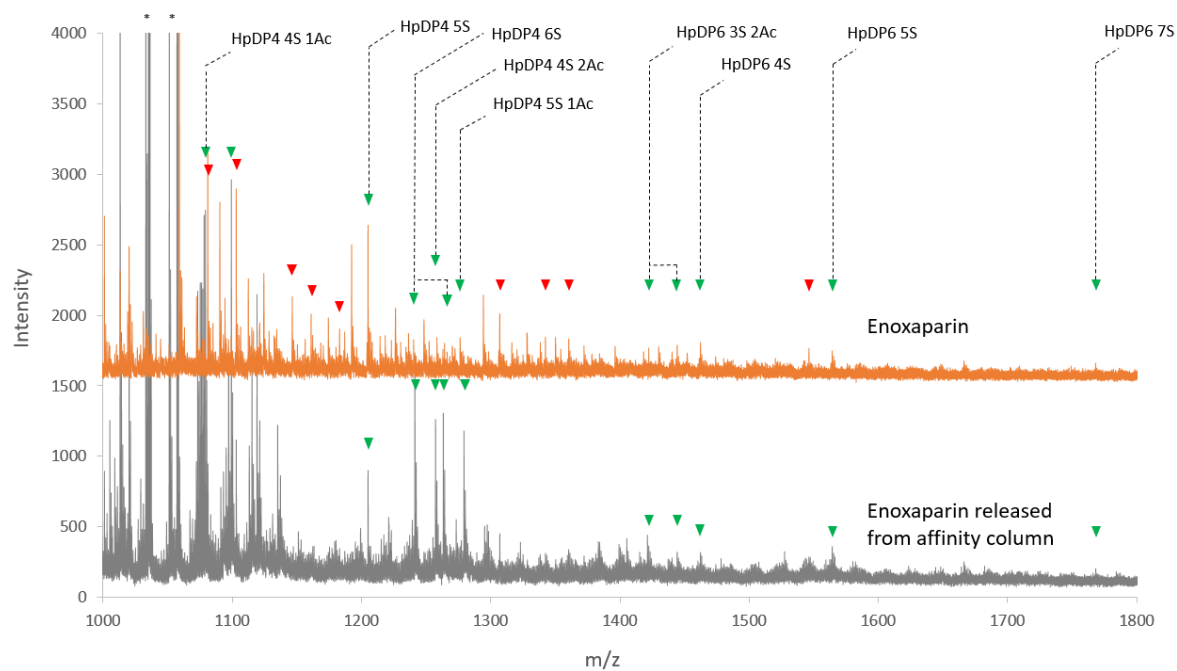


Figure 4 : Negative ion reflector MALDI-TOF mass spectrum of Enoxaparin at 200 pmol spot<sup>-1</sup> (orange line) and enoxaparin released from AT III poly(GMA-co-MBA) monolithic column (grey line). Sample were prepared with HABA/TMG ½ 80 mg mL<sup>-1</sup> in methanol matrix and a ratio 0.5 µL/1 µL of matrix/sample was deposited on AnchorChip plate.

Thus, it can be observed that the compounds selected by affinity during the capture are mainly DP4 oligosaccharide GAGs with a high degree of sulfation, although some sulfates are replaced by acetyl groups for certain chains. It can also be observed that one compound was not detected in the MALDI-TOF spectrum of intact enoxaparin. This observation tends to show that these compounds have been selected and eluted in higher concentration (relative to the other compounds). Compounds marked with red triangles in table 1 have disappeared (low affinity oligosaccharides), whereas compounds marked with green triangles have been preconcentrated (high affinity saccharides).

Increasing the ionic strength during the rinsing phase by adding a salt may improve the specificity of the capture/elution process (Figure S7). Since GAG/protein interactions are electrostatic, increasing the ionic strength may allow the elimination of oligosaccharide chains that interact mainly through electrostatic interactions but with moderate to low affinity for AT III. Some chains are eliminated by the addition of 10 mM NaCl in the washing step, while others are still detected (Table S3). The DP4 chain, containing six sulfates, is still

present during the elution step (Table 1). This chain is identified as the enoxaparin chain with the highest affinity for AT III (among those detected with sufficient sensitivity, i.e. for a DP < 8).

*Table 1: Ions identification mass spectra obtained in negative ion reflector MALDI-TOF mass spectrum of Enoxaparin at 200 pmol per spot, enoxaparin released from AT III poly(GMA-co-MBA) monolithic column with a stable and an increased ionic strength during the washing step. Sample were prepared with HABA/TMG ½ 80 mg mL<sup>-1</sup> in methanol matrix and a ratio 0.5 µL /1 µL of matrix/sample was deposited on AnchorChip plate. A cross and an empty circle corresponds respectively to presence and absence of the peak. Green arrow and red arrow correspond respectively to preservation or elimination of the signal in the released volume.*

Identification	Enoxaparin mixture	After Affinity purification	
		Washing acetate	Washing acetate + NaCl
HpDP2 2S 1Ac	⊗	▼	▼
HpDP2 3S	⊗	▼	▼
HpDP4 2S 4H	⊗	▼	▼
HpDP4 3S 3H	⊗	▼	▼
HpDP4 4S 2H	⊗	▼	▼
HpDP4 4S 1Ac 1H	○	▼	▼
HpDP4 4S 2Ac	⊗	▼	▼
HpDP4 5S 1H	⊗	▼	▼
HpDP4 5S 1Ac	⊗	▼	▼
HpDP4 6S	⊗	▼	▼
HpDP6 7S	⊗	▼	▼
HpDP6 2S 2Ac 5H	⊗	▼	▼
HpDP6 3S 6H	⊗	▼	▼
HpDP6 3S 2Ac 4H	⊗	▼	▼
HpDP6 4S 5H	⊗	▼	▼
HpDP6 4S 2Ac 3H	⊗	▼	▼
HpDP6 5S 4H	⊗	▼	▼

These results illustrate the potential of MALDI-TOF MS for the detection of enoxaparin chains in place of nanoESI-TOF MS. While this technique is less capable of providing fine structural information than ESI-MS-MS using fragmentation techniques such as Collision Induced Dissociation (CID) [36], Electron Detachment Dissociation (EDD) [37] or Negative

Electron Transfer Dissociation (NETD) [38], it can provide basic and informative data on chain length and sulfation and acetylation rates. For each detected peak, many isomers are likely to be the actual sequence, depending on the position of the sulfate substituent, or the identity of the uronic acid residue (IdoA or GlcA), as shown in Table S4. Nevertheless, among all the possible isomers, it is possible to identify probable sequences originating from the Heparin AT-binding site (pentasaccharide GlcNAc6S-GlcA-GlcNS3S6S-IdoA2S-GlcNS6S) listed in Table 2. It appears that all the hypothetical sequences share 2 to 4 monosaccharides with the known Heparin AT-binding pentasaccharide sequence. The peak detected at 1767.90 Th, attributed to HpDP6 7S, may correspond to the following sequence,  $\Delta$ UA-GlcNAc6S-GlcA-GlcNS3S6S-IdoA2S-GlcNS, which is the closest possible chain with 4 monosaccharides in common. Furthermore, the proposed sequence of the DP4 chain identified as the enoxaparin chain with the highest affinity is  $\Delta$ UA-GlcNS3S6S-IdoA2S-GlcNS6S. This sequence shares 3 monosaccharides with the heparin AT-binding site, including the 3-O-Sulfated GlcNS residue, critical in the specific AT-Heparin interaction [39]. However, the complete pentasaccharide corresponding to the AT-binding site was not detected in the released volume. It cannot be excluded that this pentasaccharide was released from the column but being fragmented during the ionisation process or being inserted in longer sequence (dp > 6) more difficult to detect into such conditions. Nevertheless, detecting and identifying affinity sequences in such a complex mixture, remains a real challenge. These results show that these affinity columns coupled with a MALDI-TOF analysis make it possible to carry out this selection, which is moreover on a miniaturized scale, drastically reducing the need for oligosaccharides and without intermediate separation technique (HILIC or SAX) thus reducing the complexity of the strategy.

Table 2: Enoxaparin sequences proposal for released chains from the AT III poly(GMA-co-MBA) monolithic column and detected by MALDI-TOF-MS compared to heparin AT-binding site. The two monosaccharides of the reducing end of the heparin AT binding site are colored in orange. The two monosaccharides of the nonreducing extremity are colored in purple. The 3OS-GlcNS residue is colored in red.

Chain	Probable Sequences	
AT binding site	GlcNAc6S-GlcA-GlcNS3S6S-IdoA2S-GlcNS6S	
Hp DP6 7S	ΔUA-GlcNAc6S-GlcA-GlcNS3S6S-IdoA2S-GlcNS	
Hp DP4 6S	ΔUA-GlcNS3S6S-IdoA2S-GlcNS6S	
HP DP4 5S 1Ac	ΔUA2S-GlcNAc6S-GlcA-GlcNS3S6S	
HP DP4 4S 1Ac 1H	ΔUA2S-GlcNAc6S-GlcA-GlcNS3S6S	
HP DP4 4S 2Ac	ΔUA2S-GlcNAc6S-GlcA-GlcNAc3S6S	
Hp DP6 5S	ΔUA-GlcNS-GlcA-GlcNS3S6S-IdoA-GlcNS	
Hp DP6 3S 2Ac	ΔUA-GlcNAc-GlcA-GlcNS3S6S-IdoA-GlcNAc	
Hp DP6 4S	ΔUA-GlcNS-GlcA-GlcNS-IdoA-GlcNS6S	



#### 4. Conclusion

This work illustrates the potential of miniaturized monolithic affinity columns grafted with AT III for the selective capture and elution of high-affinity GAG oligosaccharides in complex LMWH mixture available in minute amount. The successful release of high-affinity

compounds using ammonia 0.1M solution facilitates the characterisation of the released species by CZE and MALDI-TOF. First, the comparison of the electrophoretic profiles of enoxaparin solution before and after passing through the affinity column shows that a large proportion of the oligosaccharide sequences are eliminated during the affinity step. Then, MALDI-TOF MS allowed us to identify released sequences with a tiny volume of released sample (1 $\mu$ L) that is deposited directly onto the MALDI plate. The main sequences released from the affinity column are DP4 size length with a high degree of sulfation. These observations are consistent with the structure of the known binding pattern Fondaparinux.

However, MALDI-TOF MS allowed us to identify the size length and the number of sulfates but not their position in the oligosaccharides structure. The next steps could be to use more selective washing phases by increasing the ionic strength. On the other hand, to improve the detection of larger oligosaccharides. Indeed, the detection of oligosaccharides of size > dp6 remains difficult and it cannot be excluded that large fragments containing the interaction site were captured on the affinity column without being detected by MALDI-TOF. In addition, a depolymerisation step after capture on the column and before detection could reduce the size of the captured large dp oligosaccharides to the minimum size of the interaction site without affecting the site [15]. In addition, Coupling this methodology with structural analysis techniques, like collision induced dissociation (CID) [36], negative electron transfer dissociation (NETD) [38] or infrared multiple photodissociation (IRMPD) [40] could bring additional information.

## **Acknowledgements**

This work was supported by the Institut de Chimie de Lyon [Projet C<sup>2</sup>RTS]. We thank Jerome Lemoine for helpful discussions and assistance in the interpretation of mass spectra. We thank Charlène Bouanchaud for her help and her time spent on the MALDI-TOF MS. This

work was partially supported by the French region Rhônes Alpes Auvergne (Optolyse, CPER2016)

## References

- [1] L. Krüger, K. Biskup, V. Karampelas, A. Ludwig, A.-S. Kasper, W.C. Poller, V. Blanchard, Straightforward Analysis of Sulfated Glycosaminoglycans by MALDI-TOF Mass Spectrometry from Biological Samples, *Biology*. 11 (2022) 506. <https://doi.org/10.3390/biology11040506>.
- [2] S. Morla, Glycosaminoglycans and Glycosaminoglycan Mimetics in Cancer and Inflammation, *International Journal of Molecular Sciences*. 20 (2019) 1963. <https://doi.org/10.3390/ijms20081963>.
- [3] S.D. Vallet, O. Clerc, S. Ricard-Blum, Glycosaminoglycan–Protein Interactions: The First Draft of the Glycosaminoglycan Interactome, *J Histochem Cytochem*. 69 (2021) 93–104. <https://doi.org/10.1369/0022155420946403>.
- [4] S. Perez, O. Makshakova, J. Angulo, E. Bedini, A. Bisio, J.L. de Paz, E. Fadda, M. Guerrini, M. Hricovini, M. Hricovini, F. Lisacek, P.M. Nieto, K. Pagel, G. Paiardi, R. Richter, S.A. Samsonov, R.R. Vivès, D. Nikitovic, S. Ricard Blum, Glycosaminoglycans: What Remains To Be Deciphered?, *JACS Au*. (2023). <https://doi.org/10.1021/jacsau.2c00569>.
- [5] H.-J. Gabius, M. Cudic, T. Diercks, H. Kaltner, J. Kopitz, K.H. Mayo, P.V. Murphy, S. Oscarson, R. Roy, A. Schedlbauer, S. Toegel, A. Romero, What is the Sugar Code?, *ChemBioChem*. 23 (2022) e202100327. <https://doi.org/10.1002/cbic.202100327>.
- [6] C. Przybylski, F. Gonnet, E. Saesen, H. Lortat-Jacob, R. Daniel, Surface plasmon resonance imaging coupled to on-chip mass spectrometry: a new tool to probe protein-GAG interactions, *Analytical and Bioanalytical Chemistry*. 412 (2020) 507–519. <https://doi.org/10.1007/s00216-019-02267-2>.
- [7] L. Kjellén, U. Lindahl, Specificity of glycosaminoglycan–protein interactions, *Current Opinion in Structural Biology*. 50 (2018) 101–108. <https://doi.org/10.1016/j.sbi.2017.12.011>.
- [8] N.S. Gandhi, R.L. Mancera, The Structure of Glycosaminoglycans and their Interactions with Proteins, *Chemical Biology & Drug Design*. 72 (2008) 455–482. <https://doi.org/10.1111/j.1747-0285.2008.00741.x>.
- [9] T.H. van Kuppevelt, A. Oosterhof, E.M.M. Versteeg, E. Podhumljak, E.M.A. van de Westerlo, W.F. Daamen, Sequencing of glycosaminoglycans with potential to interrogate sequence-specific interactions, *Scientific Reports*. 7 (2017) 14785. <https://doi.org/10.1038/s41598-017-15009-0>.
- [10] M. Petitou, B. Casu, U. Lindahl, 1976–1983, a critical period in the history of heparin: the discovery of the antithrombin binding site, *Biochimie*. 85 (2003) 83–89. [https://doi.org/10.1016/S0300-9084\(03\)00078-6](https://doi.org/10.1016/S0300-9084(03)00078-6).
- [11] V.C. Hascall, The journey of hyaluronan research in the *Journal of Biological Chemistry*, *Journal of Biological Chemistry*. 294 (2019) 1690–1696. <https://doi.org/10.1074/jbc.TM118.005836>.
- [12] Y. Yu, F. Zhang, G. Renois-Predelus, I.J. Amster, R.J. Linhardt, Filter-entrapment enrichment pull-down assay for glycosaminoglycan structural characterization and protein interaction, *Carbohydrate Polymers*. 245 (2020) 116623. <https://doi.org/10.1016/j.carbpol.2020.116623>.
- [13] N. Keiser, G. Venkataraman, Z. Shriver, R. Sasisekharan, Direct isolation and sequencing of specific protein-binding glycosaminoglycans, *Nature Medicine*. 7 (2001) 123–128. <https://doi.org/10.1038/83263>.
- [14] C. Niu, Y. Zhao, C.E. Bobst, S.N. Savinov, I.A. Kaltashov, Identification of Protein Recognition Elements within Heparin Chains Using Enzymatic Foot-Printing in Solution and Online SEC/MS, *Anal. Chem*. 92 (2020) 7565–7573. <https://doi.org/10.1021/acs.analchem.0c00115>.
- [15] D. Shi, A. Sheng, C. Bu, Z. An, X. Cui, X. Sun, H. Li, F. Zhang, R.J. Linhardt, T. Zhang, L. Jin, L. Chi, A Cluster Sequencing Strategy To Determine the Consensus Affinity Domains in Heparin for Its Binding to Specific Proteins, *Anal. Chem*. 94 (2022) 13987–13994. <https://doi.org/10.1021/acs.analchem.2c03267>.
- [16] C. Zong, R. Huang, E. Condac, Y. Chiu, W. Xiao, X. Li, W. Lu, M. Ishihara, S. Wang, A. Ramiah, M. Stickney, P. Azadi, I.J. Amster, K.W. Moremen, L. Wang, J.S. Sharp, G.-J. Boons, Integrated

- Approach to Identify Heparan Sulfate Ligand Requirements of Robo1, *J. Am. Chem. Soc.* 138 (2016) 13059–13067. <https://doi.org/10.1021/jacs.6b08161>.
- [17] F. Jeanroy, C. Demesmay, V. Dugas, Miniaturized antithrombin III affinity monolithic columns coupled to TOF-MS for the selective capture and release of fondaparinux a high affinity antithrombin III ligand, *Talanta*. 241 (2022) 123275. <https://doi.org/10.1016/j.talanta.2022.123275>.
- [18] R.J. Linhardt, Heparin and anticoagulation, *Front Biosci.* 21 (2016) 1372–1392. <https://doi.org/10.2741/4462>.
- [19] L.E. Pepi, P. Sanderson, M. Stickney, I.J. Amster, Developments in Mass Spectrometry for Glycosaminoglycan Analysis: A Review, *Molecular & Cellular Proteomics*. 20 (2021) 100025. <https://doi.org/10.1074/mcp.R120.002267>.
- [20] P. Sanderson, M. Stickney, F.E. Leach, Q. Xia, Y. Yu, F. Zhang, R.J. Linhardt, I.J. Amster, Heparin/heparan sulfate analysis by covalently modified reverse polarity capillary zone electrophoresis-mass spectrometry, *Journal of Chromatography A*. 1545 (2018) 75–83. <https://doi.org/10.1016/j.chroma.2018.02.052>.
- [21] X. Han, P. Sanderson, S. Nesheiwat, L. Lin, Y. Yu, F. Zhang, I.J. Amster, R.J. Linhardt, Structural analysis of urinary glycosaminoglycans from healthy human subjects, *Glycobiology*. 30 (2020) 143–151. <https://doi.org/10.1093/glycob/cwz088>.
- [22] Z. Wang, D. Li, X. Sun, X. Bai, L. Jin, L. Chi, Liquid chromatography–diode array detection–mass spectrometry for compositional analysis of low molecular weight heparins, *Analytical Biochemistry*. 451 (2014) 35–41. <https://doi.org/10.1016/j.ab.2014.02.005>.
- [23] J. Ozug, S. Wudyka, N.S. Gunay, D. Beccati, J. Lansing, J. Wang, I. Capila, Z. Shriver, G.V. Kaundinya, Structural elucidation of the tetrasaccharide pool in enoxaparin sodium, *Analytical and Bioanalytical Chemistry*. 403 (2012) 2733–2744. <https://doi.org/10.1007/s00216-012-6045-0>.
- [24] X. Sun, Z. Guo, M. Yu, C. Lin, A. Sheng, Z. Wang, R.J. Linhardt, L. Chi, Hydrophilic interaction chromatography-multiple reaction monitoring mass spectrometry method for basic building block analysis of low molecular weight heparins prepared through nitrous acid depolymerization, *Journal of Chromatography A*. 1479 (2017) 121–128. <https://doi.org/10.1016/j.chroma.2016.11.061>.
- [25] G. Li, J. Steppich, Z. Wang, Y. Sun, C. Xue, R.J. Linhardt, L. Li, Bottom-Up Low Molecular Weight Heparin Analysis Using Liquid Chromatography-Fourier Transform Mass Spectrometry for Extensive Characterization, *Anal. Chem.* 86 (2014) 6626–6632. <https://doi.org/10.1021/ac501301v>.
- [26] K. Nimptsch, R. Süß, M. Schnabelrauch, A. Nimptsch, J. Schiller, Positive ion MALDI-TOF mass spectra are more suitable than negative ion spectra to characterize sulphated glycosaminoglycan oligosaccharides, *International Journal of Mass Spectrometry*. 310 (2012) 72–76. <https://doi.org/10.1016/j.ijms.2011.11.003>.
- [27] L. Lecas, J. Randon, A. Berthod, V. Dugas, C. Demesmay, Monolith weak affinity chromatography for  $\mu\text{g}$ -protein-ligand interaction study, *Journal of Pharmaceutical and Biomedical Analysis*. 166 (2019) 164–173. <https://doi.org/10.1016/j.jpba.2019.01.012>.
- [28] G. Zhu, H. Yuan, P. Zhao, L. Zhang, Z. Liang, W. Zhang, Y. Zhang, Macroporous polyacrylamide-based monolithic column with immobilized pH gradient for protein analysis, *ELECTROPHORESIS*. 27 (2006) 3578–3583. <https://doi.org/10.1002/elps.200600189>.
- [29] J. Gil, I. Krimm, V. Dugas, C. Demesmay, Preparation of miniaturized hydrophilic affinity monoliths: Towards a reduction of non-specific interactions and an increased target protein density, *Journal of Chromatography A*. 1687 (2023) 463670. <https://doi.org/10.1016/j.chroma.2022.463670>.
- [30] R.P. Patel, C. Narkowicz, J.P. Hutchinson, E.F. Hilder, G.A. Jacobson, A simple capillary electrophoresis method for the rapid separation and determination of intact low molecular weight and unfractionated heparins, *Journal of Pharmaceutical and Biomedical Analysis*. 46 (2008) 30–35. <https://doi.org/10.1016/j.jpba.2007.10.009>.

- [31] B.A. Williams, G. Vigh, Fast, Accurate Mobility Determination Method for Capillary Electrophoresis, *Anal. Chem.* 68 (1996) 1174–1180. <https://doi.org/10.1021/ac950968r>.
- [32] P.-E. Bodet, I. Salard, C. Przybylski, F. Gonnet, C. Gomila, J. Ausseil, R. Daniel, Efficient recovery of glycosaminoglycan oligosaccharides from polyacrylamide gel electrophoresis combined with mass spectrometry analysis, *Analytical and Bioanalytical Chemistry*. 409 (2017) 1257–1269. <https://doi.org/10.1007/s00216-016-0052-5>.
- [33] C. Przybylski, F. Gonnet, D. Bonnaffé, Y. Hersant, H. Lortat-Jacob, R. Daniel, HABA-based ionic liquid matrices for UV-MALDI-MS analysis of heparin and heparan sulfate oligosaccharides, *Glycobiology*. 20 (2010) 224–234. <https://doi.org/10.1093/glycob/cwp169>.
- [34] D. Lesur, G. Duhirwe, J. Kovensky, High resolution MALDI-TOF-MS and MS/MS: Application for the structural characterization of sulfated oligosaccharides, *Eur J Mass Spectrom (Chichester)*. 25 (2019) 428–436. <https://doi.org/10.1177/1469066719851438>.
- [35] L.E. Pepi, P. Sanderson, M. Stickney, I.J. Amster, Developments in Mass Spectrometry for Glycosaminoglycan Analysis: A Review - Molecular & Cellular Proteomics, *Molecular & Cellular Proteomics*. 20 (2021) 100025.
- [36] M.J. Kailemia, A.B. Patel, D.T. Johnson, L. Li, R.J. Linhardt, I.J. Amster, Differentiating Chondroitin Sulfate Glycosaminoglycans using CID; Uronic Acid Cross-Ring Diagnostic Fragments in a Single Stage of MS/MS, *Eur J Mass Spectrom (Chichester, Eng)*. 21 (2015) 275–285. <https://doi.org/10.1255/ejms.1366>.
- [37] J.J. Wolff, L. Chi, R.J. Linhardt, I.J. Amster, Distinguishing Glucuronic from Iduronic Acid in Glycosaminoglycan Tetrasaccharides by Using Electron Detachment Dissociation, *Anal. Chem.* 79 (2007) 2015–2022. <https://doi.org/10.1021/ac061636x>.
- [38] M. Stickney, P. Sanderson, F.E. Leach, F. Zhang, R.J. Linhardt, I.J. Amster, Online capillary zone electrophoresis negative electron transfer dissociation tandem mass spectrometry of glycosaminoglycan mixtures, *International Journal of Mass Spectrometry*. 445 (2019) 116209. <https://doi.org/10.1016/j.ijms.2019.116209>.
- [39] A. Danielsson, M.M. Kogut, M. Maszota-Zieleniak, P. Chopra, G.-J. Boons, S.A. Samsonov, Molecular dynamics-based descriptors of 3-O-Sulfated Heparan sulfate as contributors of protein binding specificity, *Computational Biology and Chemistry*. 99 (2022) 107716. <https://doi.org/10.1016/j.compbiolchem.2022.107716>.
- [40] B. Schindler, G. Laloy-Borgna, L. Barnes, A.-R. Allouche, E. Bouju, V. Dugas, C. Demesmay, I. Compagnon, Online Separation and Identification of Isomers Using Infrared Multiple Photon Dissociation Ion Spectroscopy Coupled to Liquid Chromatography: Application to the Analysis of Disaccharides Regio-Isomers and Monosaccharide Anomers, *Anal. Chem.* 90 (2018) 11741–11745. <https://doi.org/10.1021/acs.analchem.8b02801>.